

1 ***Laccaria bicolor* MiSSP8 is a small-secreted protein decisive for the**
2 **establishment of the ectomycorrhizal symbiosis**

3

4 **Clément Pellegrin^{1,2,§}, Yohann Daguerre^{1,2,☐}, Joske Ruytinx^{1,2,*}, Frédéric Guinet^{1,2},**
5 **Minna Kemppainen³, Nicolas Frei dit Frey⁴, Virginie Puech-Pagès⁴, Arnaud Hecker^{1,2},**
6 **Alejandro G. Pardo³, Francis M. Martin^{1,2} and Claire-Veneault-Fourrey^{1,2}**

7

8 **Affiliations**

9 ¹ INRA, UMR1136, Interactions Arbres/microorganismes, Centre Grand-Est, Champenoux,
10 France.

11 ² Université de Lorraine, UMR 1136, Interactions Arbres/Microorganismes (IAM), Faculté
12 des Sciences et Technologies, Vandœuvre lès Nancy, France

13 ³ Laboratorio de Micología Molecular, Departamento de Ciencia y Tecnología, Universidad
14 Nacional de Quilmes and CONICET, Roque Sáenz Peña 352, B1876 Bernal, Provincia de
15 Buenos Aires, Argentina

16 ⁴ Laboratoire de Recherche en Sciences Végétales, Université de Toulouse, CNRS, UPS, 24
17 chemin de Borde Rouge, Auzeville, BP42617, 31326, Castanet Tolosan, France.

18 § Current address: University of Cambridge, Department of Plant Sciences, Downing Street,
19 Cambridge CB2 3EA, United Kingdom.

20 ☐Current address: Umeå Plant Science Centre, Department of Forest Genetics and Plant
21 Physiology, Swedish University of Agricultural Sciences, 901 83 Umeå, Sweden

22 * Current address: Hasselt University, Centre for Environmental Sciences, Agoralaan building
23 D, 3590 Diepenbeek, Belgium

24 **Corresponding author:** claire.veneault-fourrey@inra.fr; Phone: +33 (0)383394081

25 **Keywords:** ectomycorrhizal; hyphal aggregation; repetitive motif; symbiosis; small-secreted
26 protein.

27

28 **Abstract**

29 The ectomycorrhizal symbiosis is a predominant tree-microbe interaction in forest ecosystems
30 sustaining tree growth and health. Its establishment and functioning implies a long-term and
31 intimate relationship between the soil-borne fungi and the roots of trees. Mycorrhiza-induced
32 Small Secreted Proteins (MiSSPs) are hypothesized as keystone symbiotic proteins, required
33 to set up the symbiosis by modifying the host metabolism and/or building the symbiotic
34 interfaces.

35 *L. bicolor* MiSSP8 is the third most highly induced MiSSPs in symbiotic tissues and it is also
36 expressed in fruiting bodies. The MiSSP8-RNAi knockdown mutants are strongly impaired in
37 their mycorrhization ability with *Populus*, with the lack of fungal mantle and Hartig net
38 development due to a lack of hyphal aggregation. MiSSP8 C-terminus displays a repetitive
39 motif containing a kexin cleavage site, recognized by KEX2 *in vitro*. This suggests MiSSP8
40 protein might be cleaved into small peptides. Moreover, the MiSSP8 repetitive motif is found
41 in other proteins predicted secreted by both saprotrophic and ectomycorrhizal fungi. Thus, our
42 data indicate that MiSSP8 is a small-secreted protein involved at early stages of
43 ectomycorrhizal symbiosis, likely by regulating hyphal aggregation and pseudoparenchyma
44 formation.

45

46 **Introduction**

47 Forest soils contain a wide diversity of microorganisms displaying multiple nutrition modes
48 from saprotrophy to pathogenicity, through mutualism (Buée *et al.*, 2009; Uroz *et al.*, 2010;
49 Fierer *et al.*, 2007). Tree-associated microbes are considered as key drivers of tree health,
50 productivity, and ecosystem functionality (Berg *et al.*, 2014 ; 2015). In particular, fungal
51 communities are primary contributors to carbon and nitrogen cycling in forest ecosystems
52 (van der Heijden, 1998; Lindahl and Tunlid, 2015). Trees forming ectomycorrhizae (ECM)
53 with soil-borne fungi dominate temperate and boreal forest ecosystems (Brundrett, 2009).
54 These mutualistic interactions rely on bidirectional exchanges of nutrients, which happen in
55 mycorrhized roots. The host tree provides carbon derived from its photosynthesis to the

56 fungus, whereas in return ECM fungi provide nitrogen, phosphorus and water.
57 Ectomycorrhizal fungi thus inhabit a dual ecological niche, forest soils and tree root cells,
58 requiring two contrasting ways of life: saprotrophic in soil (for nitrogen acquisition) and
59 biotrophic within plant living tissues. Therefore, most ECM fungi develop (i) extramatrical
60 mycelium exploring the rhizospheric surrounding soil, (ii) aggregated fungal hyphae
61 ensheathing fine lateral roots named mantle, and finally (iii) a highly branched network of
62 fungal hyphae (called the Hartig net) within the apoplastic space of epidermal and cortical
63 root cells (Martin *et al.*, 2016). The Hartig net constitutes the biotrophic interface required for
64 efficient nutrient exchanges. In particular environmental conditions (humidity, temperature),
65 host-derived carbon can be used to build the fruiting body, a spore-releasing structure made of
66 hyphal aggregation (Kües and Navarro-González, 2015; Genre and Bonfante, 2012;
67 Lakkireddy *et al.*, 2011).

68 Despite their critical ecological roles, only a few ECM interactions have been studied at the
69 molecular level. Notably, mechanisms mediating the early steps of ECM symbiosis
70 development remain mostly uncharacterized (Daguette *et al.*, 2017; Martin *et al.*, 2016). First,
71 a pre-contact phase during which plant and fungi communicate is a prerequisite for successful
72 root colonization. Diffusible molecules such as fungal auxins and sesquiterpenes likely
73 mediate this communication and trigger an increase in the lateral roots formation (Felten *et al.*,
74 2009; Ditengou *et al.*, 2015; Krause *et al.*, 2015; Vayssières *et al.*, 2015). Then, fungal
75 accommodation within the apoplast of root cells requires controlling both hyphal and host
76 root development (Martin *et al.*, 2016). For example, in the poplar-*L. bicolor* model, both
77 ethylene and jasmonic acid treatments restrain *in planta* fungal colonization i.e. restrict the
78 intradical hyphal network (Plett *et al.*, 2014). The symbiotic interface at the Hartig net derives
79 from remodeling of both fungal and plant cell walls (Balestrini and Kottke, 2016). Cell wall
80 carbohydrates and proteins (e.g. hydrophobins, mannoproteins) are thus likely to actively
81 contribute to *in planta* fungal colonization (for review, Balestrini and Kottke, 2016) and to
82 efficient nutrient exchanges. Formation of the Hartig net also leads to a massive fungal
83 colonization within the apoplast of colonized roots, without eliciting strong defence responses
84 (Martin *et al.*, 2016). Considering ECM symbiosis as a biotrophic plant-fungal interaction,

85 secreted fungal molecules likely govern plant colonization by subverting host immunity and
86 manipulating its metabolism to promote the symbiosis establishment and/or functioning (Plett
87 and Martin, 2015; Lo Presti *et al.*, 2015).

88 Genome-wide analysis of *Laccaria bicolor* has led to the identification of 98 proteins, named
89 MiSSPs (Mycorrhiza-induced Small Secreted Proteins), up-regulated in symbiotic tissues
90 (Martin *et al.*, 2008). Among them, only MiSSP7 has been described as a symbiosis effector
91 so far. MiSSP7 is secreted by the fungus and it enters the host cells in which it localizes
92 within the nucleus. Moreover, *MiSSP7-RNAi* mutants are impaired in ectomycorrhiza
93 formation (Plett *et al.*, 2011). Inside the nucleus, MiSSP7 interacts with the *Populus*
94 *trichocarpa* PtJAZ6 (JAsmonate Zim domain 6), a co-receptor of jasmonic acid (Plett *et al.*,
95 2014). MiSSP7 stabilizes PtJAZ6, avoiding its degradation in the presence of jasmonic acid,
96 leading to the repression of target genes' transcription (Plett *et al.*, 2014). Preliminary results
97 have shown that genes involved in plant cell wall remodelling and plant defence responses
98 might be these target genes (Plett *et al.*, 2014). Furthermore, effector proteins, such as SP7
99 from the arbuscular mycorrhizae fungus *Rhizophagus irregularis* (Kloppholz *et al.*, 2011), as
100 well as PIIN_08944 and FGB1 (Fungal Glucan-Binding 1, PIIN_03211) from the root
101 endophyte *Piriformospora indica* (Akum *et al.*, 2015; Wawra *et al.*, 2016) also suppress host
102 immunity promoting root colonization and symbiosis. These data support the concept
103 whereby a mutualistic symbiont uses its repertoire of secreted proteins to set up the symbiosis
104 by suppressing host immunity and/or targeting cell-wall remodeling.

105 Considering the diversity of secreted proteins used by pathogens to alter the host metabolism,
106 mycorrhizal fungi might use an equivalent strategy to setup their interaction. However,
107 available literature on such proteins required for the symbiosis establishment is still very poor
108 and functional analyses of MiSSPs are required to clarify and detail how mycorrhizal fungi
109 communicate with their host plant to establish interaction (Plett and Martin, 2015). The
110 Mycorrhiza-induced Small Secreted Protein of 8 kDa, i.e MiSSP8 (JGIv2 ID #388224),
111 displays the third highest induction in mature ectomycorrhizal root tips and is also up-
112 regulated in fruiting-bodies (Martin *et al.*, 2008). MiSSP8 is, with other MiSSPs, part of the
113 “core” regulon expressed during the colonization of two hosts, *Populus trichocarpa* and

114 *Pseudotsuga menziesii* (Plett *et al.*, 2015). The proteins associated to this core regulon have
115 hence been hypothesized to be the key genetic determinants required for the symbiosis
116 development in *L. bicolor* (Plett *et al.*, 2015). In this study, we report the functional analysis
117 of *L. bicolor* MiSSP8 by using a combination of experimental and *in silico* approaches. Here,
118 we identify MiSSP8 as a key symbiosis factor required for *L. bicolor* mycorrhization ability,
119 mantle formation and subsequent Hartig net development. This symbiosis factor also has a
120 repetitive motif at its C-terminus containing a kexin-like cleavage site, which is recognized by
121 KEX2 *in vitro* and liberate four short peptides. The repetitive motif of MiSSP8 is found in
122 other fungal proteins, mostly from ECM and saprotrophic fungi. All together our data indicate
123 that MiSSP8 is involved in fungal mantle and Hartig net formation, potentially by regulating
124 hyphal aggregation, and suggest a part of the symbiotic toolbox used by the ECM fungi to
125 initiate symbiosis is already present in the genome of their saprotrophic ancestors.

126

127 **Material and methods**

128 ***Microorganism and plant material***

129 *Saccharomyces cerevisiae* strains YTK12 (Jacobs *et al.*, 1997), MaV103 and MaV203
130 (Invitrogen) were propagated in YAPD medium (1% yeast extract, 2% peptone, 2% glucose,
131 and 40 mg/L adenine) and cultured at 30°C. The ectomycorrhizal fungus *L. bicolor* Maire P.
132 D. Orton strains (S238N and RNAi-lines) were maintained at 25°C on modified Pachlewski
133 medium P5 +/- 150µg.ml⁻¹ of hygromycin B (Pachlewski and Pachlewska, 1974, Di Battista
134 *et al.*, 1996). The hybrid *Populus tremula x Populus alba* (INRA clone 717-1-B4) cuttings
135 were micropropagated *in vitro* and grown on half MS medium (Murashige and Skoog, 1962)
136 in glass culture tubes under a 16 h photoperiod at 24°C in a growth chamber. *L. bicolor*
137 basidiocarps were harvested beneath inoculated Douglas fir in a nursery. Three fruiting body
138 samples from two developmental stages were harvested ; the “early” stage corresponding to
139 just emerging fruiting body and “late” stage corresponds to ones with “open” cap. Samples
140 from both developmental stages were divided into stipe and cape prior to RNAs extraction
141 (Fig. S1).

142 To test for altered cell wall susceptibility, Congo red (150 µg/mL; Sigma-Aldrich) was added

143 to the medium (Fig. S2).

144

145 ***Yeast secretion trap assay***

146 Functional validation of the predicted signal peptide of MiSSP8 was done using the yeast
147 signal-sequence trap assay (Plett *et al.*, 2011). Briefly, full-length sequences of MiSSP8 with
148 or without its signal peptide were cloned into pSUC2-GW, a plasmid carrying the invertase
149 *SUC2* lacking both its initiation methionine and signal peptide. Yeast strain YTK12 was
150 transformed with 200 ng of the plasmid using the lithium acetate method (Gietz and Schiestl,
151 2008). All transformants were confirmed by PCR with vector-specific primers and grown on
152 yeast minimal medium with glucose (SD-W medium: 0.67% Yeast Nitrogen Base without
153 amino acids, 0.075% tryptophan dropout supplement, 2% glucose and 2% agar). To assess
154 invertase secretion, overnight yeast cultures were diluted to an $O.D_{600} = 1$ and 20 μ l of
155 dilution were plated onto YPSA medium (1% yeast extract, 2% peptone, 2% sucrose, and 1
156 μ g.mL⁻¹ antimycin A, inhibitor of cytochrome c oxidase). The YTK12 strains transformed
157 with either the pSUC2-GW empty vector or containing SUC2SP (yeast invertase with signal
158 peptide) were used as negative and positive controls, respectively.

159

160 ***Genetic transformation of *L. bicolor****

161 The *ihpRNA* expression cassette/transformation vector was constructed using the
162 pHg/SILBA γ vector system (Kemppainen *et al.*, 2005; Kemppainen and Pardo, 2009). The
163 full-length MiSSP8 cDNA was amplified from oligo(dT)18 synthesized S238N cDNA (First
164 Strand cDNA Kit, (Fermentas) using the following gene specific primers:

165 MISSP8-*Sna*BIFor: CTTCTACGTAATGTATTTCCACACTCTTTTCG

166 MISSP8-*Hind*IIIRev: TGTC AAGCTTTCAATCACTATCGCGCCTC.

167 The cDNA was TA-cloned into pCR®2.1-TOPO® (Invitrogen) for sequencing and the
168 corresponding plasmid was used as PCR template to obtain the amplicons needed for *ihpRNA*
169 expression cassette construction. The cloning into the pSILBA γ vector was carried out using
170 the *Sna*BI, *Hind*III, *Bgl*II and *Stu*I restriction sites in pSILBA γ . Primers used for
171 amplification of the MiSSP8 sequence arms were:

172 MISSP8-*Sna*BIFor: CTTCTACGTAATGTATTTCCACACTCTTTTCG

173 MISSP8-*Hind*IIIRev: TGTC AAGCTTTCAATCACTATCGCGCCTC

174 MISSP8-*Bgl*IIRev: TGTCAGATCTTCAATCACTATCGCGCCTC

175 Completed ihpRNA expression cassette was further cloned as a full length *Sac*I linearized
176 pSILBAy plasmid into the T-DNA of the binary vector pHg to create pHg/pS γ MiSSP8. The
177 pHg/pS γ MiSSP8 was used for transforming *L. bicolor* dikaryotic strain S238N with
178 *Agrobacterium tumefaciens* strain AGL1 (Kempainen and Pardo, 2005). The transformed
179 fungal strains were selected with 300 $\mu\text{g.mL}^{-1}$ hygromycin B (Invitrogen) and were later
180 maintained under 150 $\mu\text{g.mL}^{-1}$ hygromycin B selection pressure on modified P5 medium.
181 Four pHg/pS γ MiSSP8 *L. bicolor* transformant strains were used for further molecular and
182 physiological analyses.

183

184 ***Molecular analyses of Laccaria bicolor transformants***

185 Plasmid rescue of the right border (RB) - linked gDNA was carried out with BamHI cut and
186 self-ligated *L. bicolor* gDNA according to Kempainen *et al.* (2008). Sequencing of the
187 rescued plasmids was done using M13/pUC-reverse primer (-26)17 mer. Left border (LB)
188 TAIL-PCR was done according to Kempainen *et al.*, 2009, using three T-DNA specific
189 nested primers LB1.3 (Mullins *et al.*, 2001) and the arbitrary primer AD2 (Liu *et al.*, 1995).
190 L3/AD2 amplified TAIL-PCR products were TA-subcloned into pCR $\text{\textcircled{R}}$ 2.1-TOPO $\text{\textcircled{R}}$
191 (Invitrogen) and sequenced with the L3 primer. All the PCR reactions were carried out using
192 Tpersonal thermocycler (Biometra $\text{\textcircled{R}}$) and PCR chemicals from Fermentas. Sequencing
193 reactions were purchased from Macrogen Sequencing Service (Seoul, SK).

194

195 ***In vitro mycorrhization experiments***

196 For *in vitro* mycorrhization tests between *P. tremula x alba* INRA717-1B4 and *L. bicolor*, we
197 used a “sandwich” co-culture system described in Felten *et al.* (2009). After three weeks of
198 co-incubation of poplar cuttings with *L. bicolor*, at least 10 to 20 biological replicates were
199 analysed for the percentage of colonized roots with the *L. bicolor* wild-type strain S238N or
200 with the four *L. bicolor* MiSSP8-RNAi lines. Two independent empty vector transformants of

201 *L. bicolor* (ev7 and ev9 lines, Plett *et al.*, 2011) were also tested for their ability to colonize
202 roots.

203 ***Motif analysis***

204 For the identification of proteins sharing the DWRR motif found in MiSSP8 sequence, the
205 following regular expression

206 DW[K/R]-x(2,20)-DW[K/R]-x(2,20)-DW[K/R]-x(2,20)-DW[K/R]-x(2,20) was used on a set
207 (Table S1) of fungal and oomycete proteomes available at the MycoCosm database (March
208 2019) using the PS-Scan software (de Castro *et al.*, 2006) with the options -g (greedyness off)
209 -v (overlaps off) -p (pattern search). Only protein sequences from published genomes starting
210 with a methionine were kept for further analysis (Table S1). In order to assess conservation of
211 the DWRR motif, protein sequences retrieved by PS-Scan were further analyzed by GLAM2
212 (Gapped Local Alignments Motifs) software v 4.11.0 (Frith *et al.*, 2008) with default
213 parameters. Similar GLAM2 analysis was performed on shuffled sequences as control. The
214 presence of a signal peptide in the protein sequence was assessed with SignalP v 4.1 (Petersen
215 *et al.*, 2011) with default parameters.

216

217 ***Microscopy analysis of poplar-ECM roots.***

218 ECM root tips of *poplar-L. bicolor* (WT or *MiSSP8*-RNAi lines) were fixed 24 h in 4%
219 paraformaldehyde in PBS buffer (100 mM phosphate buffer, 2.7 mM KCl and 137 mM NaCl
220 pH 7.4) at 4°C. The root segments were embedded in agarose 5% and cut into 25 µm radial
221 sections with a Leica VT1200S Leica vibratome (Leica Microsystems). Sections were
222 categorized according to their distance (100, 200 and 600 µm) from the root apex. 25 µm-
223 width sections were stained with 10µg.mL⁻¹ wheat germ agglutinin (WGA)–Alexa Fluor®
224 488 Conjugate (W21404, ThermoFisher, France) and 1µg.mL⁻¹ propidium iodide (Invitrogen,
225 France). To compare the development of the Hartig net between samples, sections between
226 200 and 600 µm distance from the root apex were analyzed.

227

228 ***Cell imaging by confocal laser-scanning microscopy***

229 Transversal sections of ECM root tips were viewed by a Zeiss LSM780 (Carl Zeiss AG,
230 Germany) confocal laser scanning microscope system. Images were obtained with objective
231 CAPO-40x/1.2 water-immersion objective, acquired sequentially to exclude excitation and
232 emission crosstalk (when required). Spectral deconvolution was used to assess specificity of
233 the emission signal. Images were processed with ZEN (Carl Zeiss AG) software.

234

235 ***Quantitative RT-PCR***

236 For the expression of *MiSSP8* in colonized root tips, extramatrical and free-living mycelium,
237 total RNA was extracted from 100 mg biological material using the RNeasy Plant Mini Kit
238 (Qiagen), extraction buffer RLC was supplemented with 2% PEG8000. An on column DNase
239 I treatment was included in the protocol. 500 ng of total RNA was converted into cDNA in a
240 20 μ l reaction using the High-Capacity cDNA Reverse Transcription Kit (Applied
241 Biosystems, Life technologies, Thermo Fisher Scientific) according to manufacturer's
242 instructions and subsequently 1/5 diluted in sterile RNase and DNase free water. Real-time
243 qPCR was performed in an optical 96-wells plate with a StepOne sequence detection system
244 (Applied Biosystems, Life Technologies) and fast cycling conditions (20 s at 95°C, 40 cycles
245 of 3 s at 95°C and 30s at 60°C). Each 10 μ l reaction contained 2X Fast SYBR green Master
246 Mix (Applied Biosystems, Life Technologies), 300 nM gene-specific forward and reverse
247 primers, water and 10 ng of cDNA. Data were expressed relatively to the sample with the
248 highest expression level ($2^{-Ct-Ct_{min}}$) and normalized against six reference genes (JGIv2 IDs
249 #293350, #611151, #313997, #446085, #246915 and #319764). Stability of the reference
250 genes was confirmed by geNorm analysis (Vandesompele *et al.*, 2002). The normalization
251 factor NF for each sample was calculated as the geometric mean of the relative expression
252 level of the six reference genes. Consequently, the expression level of *MiSSP8* for an
253 individual sample was obtained by the formula $2^{-Ct-Ct_{min}}/NF$ according to Vandesompele *et*
254 *al.* (2002). Finally, data were rescaled relative to the FLM.

255 For the fruiting body expression, cDNA was obtained from 500 ng of total RNA using the i-
256 Script cDNA reverse transcription kit (Biorad) in a final volume of 20 μ L. RT-qPCR
257 reactions were performed on 10 ng cDNA and 300 nM forward and reverse primers in each

258 reaction, using the RotorGene (Qiagen) with the standard cycle conditions: 95 °C for 3 min;
259 40 cycles at 95 °C for 15 s and 65 °C for 30 s, followed by a melting curve analysis
260 (temperature range from 65 °C to 95 °C with 0.5 °C increase every 10 s). In this particular
261 case, transcript abundance was normalized using *L. bicolor* histone H4 (JGIv2 ID# 319764)
262 and ubiquitin (JGIv2 ID #446085) encoding genes. Amplification efficiency (E) was
263 experimentally measured for each primer pair and was taken in account for calculation of
264 normalized expression (Pfaffl *et al.*, 2001).

265

266 ***Production of recombinant protein and biochemical analysis***

267 *MiSSP8Δ1-20* (i.e. devoid of its first twenty amino-acid residues) was synthesized by
268 Genecust (Luxembourg) and subcloned into the pET-28a-CPDSalI vector (Shen *et al.*, 2009)
269 between *NcoI* and *SalI* restriction sites. The resulting plasmid was subsequently used for the
270 transformation of the Rosetta2 (DE3) pLysS strain of *E. coli* (Novagen). The expression of
271 the recombinant protein (ending with DSDVD in C-ter) was performed at 37°C in Lysogeny
272 broth (LB) medium supplemented with 30 µg.mL⁻¹ of kanamycin and 34 µg.mL⁻¹ of
273 chloramphenicol. When the cell culture reached an O.D₆₀₀ of 0.7, recombinant protein
274 expression was induced by the addition of 0.1 mM isopropyl β-D-1-thiogalactopyranoside
275 (IPTG), and the cells were grown for further 4 hours at 37°C. Cells were then harvested by
276 centrifugation (13000rpm, 5min), resuspended in a 30 mM Tris/HCl pH 8.0, 200 mM NaCl
277 lysis buffer and lysed by sonication. The cell extract was centrifuged at 35000 g for 25 min at
278 4°C to remove cellular debris and aggregated proteins. C-terminal His-tagged proteins were
279 purified by gravity-flow chromatography on a nickel nitrilotriacetate (Ni-NTA) agarose resin
280 (Qiagen) according to the manufacturer's recommendations followed by an exclusion
281 chromatography on a Superdex75 column connected to an ÄKTA Purifier™ (GE Healthcare).
282 CPD-tag was cleaved using 200 µM inositol-6-phosphate as described by Schen *et al.* (2009)
283 and removed by size exclusion chromatography. Circular dichroism experiments were carried
284 out with 75 µM of recombinant MiSSP8 in 10 mM sodium phosphate buffer pH 7 using a
285 Chirascan Plus (Applied Photophysics).

286

287 ***In vitro* digest assay of recombinant MiSSP8 by KEX2.**

288 Recombinant MiSSP8 protein (75µg) was incubated with 0.02 units of recombinant KEX2
289 protease (MoBiTec) in 5 mM CaCl₂, 50 mM Tris pH7 at room temperature during 1, 2, 4 or 6
290 hours then was stopped by heating at 95°C for 10 minutes. 50% of each samples was analysed
291 on Tris-Tricine-precast 12-15% polyacrylamide gels (Biorad), stained with Coomassie blue.
292

293 **Mass spectrometry analysis using LC Q-TRAP of KEX2-digested MiSSP8.**

294 Synthesized peptide standard (DSDW) obtained from Genecust was solubilized and diluted to
295 10⁻⁸M in 2% acetonitrile in water and stored at -20°C. *In vitro* KEX2/MiSSP8 digest assay
296 was diluted in 100 µl of 2% acetonitrile in water and stored at -20°C. The U-HPLC 3000
297 (Dionex) was equipped with a reverse-phase column Acquity UPLC BEH-C18 (2.1 x 150
298 mm, 1.7 µm, Waters). Separation was done with a gradient of eluent A (water/0.1% formic
299 acid) and eluent B (acetonitrile), started at 5% B for 1 min, followed by a 8 min gradient to
300 100% B, followed by an isocratic step at 100% B for 2 min, a 2 min gradient back to 5% B,
301 equilibration step 2 min at 5% B, before starting another analysis, at a constant flow rate of
302 300µl/min. 10µl of each samples were injected.

303 The mass spectrometer used was a 4500 Q-Trap mass spectrometer (Applied Biosystems,
304 Foster City, USA) with an electro-spray ionization source in the positive ion mode. The
305 capillary voltage was fixed at 4500 V and the source temperature at 400°C. Optimizations of
306 the source parameters were done using the peptide standards DSDW at 10⁻⁵ M in 2 %
307 acetonitrile by infusion at 7µl. min⁻¹, using a syringe pump. For MS/MS analysis, enhanced
308 product ions (EPI) mode was used. Declustering potential was fixed at 110 V. Fragmentations
309 were induced by collision induced dissociation (CID) with nitrogen at a collision energy of 40
310 V. For the multiple reaction monitoring (MRM) mode, each precursor ions and b/y ions were
311 calculated for the predicted peptide using Protein Prospector. For relative quantification, the
312 transitions selected for each peptide were: 522.5>185 (DSDW, RT: 5.0 min), 550.5>175
313 (DSDVD, RT: 4.5 min), 678.5>254 (RDSDW, RT: 5.0 min), 678.5>361 (DSDWR, RT: 4.4
314 min), 834.5>517 (DSDWRR, RT: 4.0 min), 834.5>361 (RDSDWR, RT: 4.0 min), 834.5>313

315 (RRDSDW, RT: 4.0 min). The intensity of peak height was measured in counts per second
316 (cps).

317

318

319 **Results**

320

321 ***MISSP8* is up-regulated both in ECM root tips and fruiting body.**

322 Transcript profiling of *L. bicolor* free-living mycelium and *P. trichocarpa* colonized root tips
323 have highlighted the presence of >50 Mycorrhiza-induced Small Secreted Proteins (MiSSPs)
324 in this ECM fungus. Of these, *MiSSP8* displayed the third highest induction in mature
325 ectomycorrhizal root tips (Martin *et al.*, 2008). To determine the regulation of *MiSSP8*
326 throughout ECM development, we investigated *MiSSP8* expression during *in vitro* ECM time
327 course with *P. tremula x alba* using real time-qPCR. At 7 days post-contact, fungal hyphae
328 started colonization of fine roots and form the mantle. At 14 days, the Hartig net is present
329 and at 21 days, fully mature ECM tissues have developed. The very low and constitutive-level
330 of *MiSSP8* expression in free-living mycelium (FLM) was set as a reference. *MiSSP8* was up-
331 regulated in ECM root tips from day 7 to day 14, reaching its maximum induction at this latter
332 time point (Fig. 1A). The expression decreased to reach the same level as in FLM at 21 days
333 (mature ECM). Expression of *MiSSP8* in the extraradical mycelium (i.e. the part of the
334 rhizospheric mycelium not in contact with the roots) was the same as FLM all along the time
335 course (Fig. 1A). In order to investigate the expression level of *MiSSP8* in a non-symbiotic
336 tissue, we performed qRT-PCR on *L. bicolor* fruiting body tissues (stipe and cap) at two
337 different developmental stages (early and late) (Fig. 1B, Fig. S1). The expression of *MiSSP8*
338 in *L. bicolor* sporocarps is higher than its expression in FLM and ECM root tips. Overall,
339 *MiSSP8* was strongly induced during fruiting body-development and *P. tremula x alba* root
340 colonization (mantle and Hartig net formation).

341

342 ***MiSSP8* is secreted as indicated by the yeast invertase secretion assay**

343 MiSSP8 is a protein containing 70 amino acids, the first twenty residues of which encode a
344 predicted signal peptide as predicted by SignalP v4.1 (Fig. 1C). According to the
345 hydrophobicity plot, the mature MiSSP8 is a hydrophilic protein with charged amino acids
346 exposed to solvent (Fig. 1C) but there is no predicted secondary structure (Fig. S2A). A
347 circular dichroism experiment performed on the recombinant protein produced in *E. coli*
348 further confirms the lack of secondary structure of MiSSP8 (Fig. S2B). In order to confirm
349 that the predicted signal peptide is functional and properly processed, the full length MiSSP8
350 (including its signal peptide) was fused to the yeast invertase *SUC2*, which catalyzes the
351 hydrolysis of sucrose. The transformed yeasts were able to grow on a minimal medium
352 supplemented with sucrose and antimycin (Fig. 1D, bottom right) like the yeast transformed
353 with a full-length invertase (Fig. 1D, bottom left). Yeasts transformed with an empty vector
354 control (Fig. 1D, top left) or an invertase fused to MiSSP8 lacking its signal peptide (Fig. 1D,
355 top right) did not grow on the same medium. This demonstrates that the signal peptide of
356 MiSSP8 is properly recognized and processed in yeast and triggered the secretion of the
357 invertase. Therefore, it is likely that *L. bicolor* secretes MiSSP8 into the extracellular space
358 during root colonization and fruiting body development.

359

360 **MiSSP8-repetitive motif is shared with proteins containing repeats from saprotrophic** 361 **and ectomycorrhizal fungi**

362

363 The mature MiSSP8 is composed of 50 amino acids, with a predicted molecular weight of
364 6105.32 Da and a theoretical pI of 5.12. At its C-terminus, MiSSP8 contains a 25 amino acids
365 long sequence carrying a repetitive motif (i.e. DWRR), repeated four times consecutively.
366 This protein displayed sequence similarities with only one protein of *Laccaria amethystina*
367 (JGIv2 #676588), a close relative of *L. bicolor*, according to BLASTP search on NCBI and
368 JGI MycoCosm databases. Altogether, these data suggest that MiSSP8 is a natively
369 unstructured protein without sequence similarities with previously characterized proteins. To
370 identify additional proteins with a similar motif at their C-termini, we used a pattern search
371 algorithm and identified in total 38 proteins from 23 published fungal proteomes (Fig. 2,

372 Table S1). The DW[K/R]R containing proteins identified were mostly associated to
373 saprotrophs (32/38) and ectomycorrhizal (5/38) fungi including also one arbuscular
374 mycorrhizal fungus, but none pathogenic fungi (Fig. 2, Table S1). Most of the proteins
375 identified above using pattern search algorithm (34/38) had a predicted signal peptide (Fig. 2).
376 No protein domains were detected by PROSITE database, except for two proteins from the
377 white rot fungus *Schizophyllum commune*, which possess a N-terminal aspartic peptidase A1
378 domain (Fig. 2). GLAM2 motif analysis found an enrichment of a DWR/KR motif, named
379 DW[K/R]R thereafter.

380 The median size of the proteins was 138.5 amino acids, ranging from 70 to 738 amino acids
381 (Fig. 3A). The number of repetitions of the conserved peptide varied from three to seventeen,
382 with no correlation between the size of the protein and the number of motifs (Fig. 3B, Fig.
383 S3). RNA-Seq expression data from *Pinus pinaster* root tips colonized by the ectomycorrhizal
384 fungus *Hebeloma cylindrosporum* showed that the DWRR containing protein from *H.*
385 *cylindrosporum* (JGI IDv2: 440029) was upregulated during root colonization (Doré *et al.*,
386 2015; GEO accession number GSE63868/GSE66156). GLAM2 motif analysis found an
387 enrichment of a DWR/KR motif, named DW[K/R]R thereafter (Fig. 3C, Fig. S3). The
388 DW[K/R]R repetitive motif is therefore shared between proteins predicted as secreted for the
389 most part and associated to saprotrophs and mycorrhizal fungi.

390

391 **MiSSP8 possess a repetitive motif containing a kexin cleavage site, recognized *in vitro* by**
392 **the yeast KEX2 protease.**

393 The presence of a repetitive motif in the protein sequence suggests that MiSSP8 might be
394 processed post-translationally in order to become active. Interestingly, the motif DW[K/R]R
395 contains [K/R]R residues, which are known recognition sites for KEX2 proteases in fungi
396 (Mizuno *et al.*, 1988; Mizuno *et al.*, 1989). In fungi, an additional proteolytic cleavage of the
397 KEX2-peptides occurs by KEX1 to withdraw the two amino acids KR or RR. The processing
398 of MiSSP8 at the identified cleavage sites (i.e. RR at each DWRR repeats) by KEX1 and
399 KEX2 would release one peptide of 27 amino acids, three short peptides of four amino acids
400 (DSDW) and a final three amino acids long peptide DSD. The sole action of the KEX2

401 protease will lead to the release of the DSDWRR peptide. In order to assess whether this
402 motif is recognized by KEX2, we performed *in vitro* digest assay of recombinant mature
403 MiSSP8 with recombinant yeast KEX2 protein. MiSSP7, a *L. bicolor* small-secreted protein
404 of 7kDa, which does not contain the (K/R)R motif, was used as negative control. After 2h of
405 incubation, the amount of undigested MiSSP8 decreased and was not detectable after 4h of
406 incubation. For the same incubation period, MiSSP7 was not degraded (Fig. 4). Using mass
407 spectrometry, we assessed whether the predicted DSDWRR or additional peptides were
408 produced to confirm the specificity of the *in vitro* enzyme test. The separation and analytical
409 detection parameters by mass spectrometry were fixed using the synthetic standard DSDW.
410 We obtained a limit of detection of the standard DSDW at 10^{-8} M for 10 μ l injected, at a
411 retention time of 5.08 min. In the products of digestion, we searched for C-terminal DSDVD,
412 the peptide DSDW and other predicted peptides with one to two additional arginine (R)
413 before/after DSDW (Figure 1C). Among the major detected peptides, we observed the C
414 terminal peptide DSDVD, DSDWR and DSDWRR, meaning that as predicted, KEX2 can
415 hydrolyze MiSSP8 after two arginines (formation of DSDVD and DSDWRR), and between
416 the two remaining arginines, to form DSDWR (Fig. S4).

417

418 **RNAi-mediated knockdown of MiSSP8 encoding gene impairs mycorrhization rate**

419 Since *MiSSP8* expression is induced during the early steps of ectomycorrhizal symbiosis
420 development, we assessed whether MiSSP8 is required for establishment of symbiotic
421 interaction. Generation of knockout mutants through homologous recombination has not been
422 accomplished so far in *L. bicolor*. However, genetic tools to obtain *L. bicolor* strains with
423 significantly reduced target gene expression levels through RNA interference (RNAi) are
424 available (Kemppainen *et al.*, 2009; Kemppainen and Pardo 2010). RNAi hairpin targeting
425 the MiSSP8 transcripts was expressed in *L. bicolor* through *A. tumefaciens* mediated
426 transformation (ATMT). A transgenic ATMT *Laccaria* library was generated and 24
427 randomly selected independent RNAi lines were passed through consecutive hygromycin B
428 selection steps. Among these, four *Laccaria* RNAi lines were analyzed at molecular level
429 (Plett *et al.*, 2011; Table S2). Real-time qPCR analysis confirmed down-regulation of *MiSSP8*

430 in the four transgenic lines, with a reduction from 82% to 95% compared to the empty-vector
431 control lines (Fig. 5A). We quantified the ability of these transgenic RNAi lines to colonize *P.*
432 *tremula x alba* roots *in vitro*. The mycorrhization rate, defined as percentage of ECM root tips
433 formed over the total number of lateral roots, was found significantly reduced with the
434 mutants, being 45% for the wild-type and empty-vector controls and only 10 to 15% for the
435 four *L. bicolor* *MiSSP8*-RNAi lines (Fig. 5B). The mycelial growth of each of the *MiSSP8*-
436 RNAi line was tested on rich agar medium or on Congo Red-containing medium and it was
437 similar to the wild-type strain S238N (Fig. S5). Neither did the RNAi mutant show any
438 growth defect nor altered fungal cell wall susceptibility compared to the wild-type fungus.
439 Altogether, it demonstrates *MiSSP8* is required for the establishment of the symbiosis with
440 poplar.

441

442 **RNAi-mediated knockdown of *MiSSP8* impairs formation of fungal mantle and** 443 **subsequent Hartig net development**

444 To estimate whether *MiSSP8* is necessary for fungal mantle and Hartig net development (two
445 hallmarks of the mature ectomycorrhizal root tips), we performed microscopy analysis on
446 ECM poplar root tips formed. After one week of contact with poplar roots, the fungal mantle
447 formed by *MiSSP8*-RNAi lines was strongly unstructured and thinner than the one obtained
448 with the reference strain (empty vector (ev) control). In addition, whereas ev control already
449 formed first steps of Hartig net, the *MiSSP8*-RNAi lines did not display any kind of fungal
450 colonization. After two weeks, *MiSSP8*-RNAi lines displayed one or two layers of fungal
451 hyphae forming the mantle (Fig. 5C). This observation contrasts with the fungal mantle
452 formed with the control transformant strain, which displayed a thick and well-organized
453 fungal sheath with several layers of fungal hyphae stacked on each other. More strikingly,
454 *MiSSP8*-RNAi lines were impaired in their ability to form the Hartig net even after two weeks
455 of contact (Fig. 5C). Altogether, these results highlight the involvement of *MiSSP8* in the
456 differentiation of the fungal mantle precluding hyphal expansion to form the Hartig net.

457

458 **Discussion**

459 **MiSSP8 is required for symbiosis development, likely through its role for hyphal**
460 **aggregation.**

461 Several MiSSPs from *L. bicolor*, including MiSSP8, are known to be part of the “core”
462 regulon expressed during the colonization of two hosts, *Populus trichocarpa* and *Pseudotsuga*
463 *menziesii* (Plett *et al.*, 2015). These proteins have hence been hypothesized to be key genes
464 required for the symbiosis development in *L. bicolor* (Plett *et al.*, 2015). The strong decrease
465 in the ability to form mycorrhizae by the *MiSSP8*-targeted RNAi lines is consistent with this
466 hypothesis. In addition, our study clearly shows that MiSSP8 is directly involved in the
467 symbiosis establishment, through a role played in mantle formation and the subsequent Hartig
468 net development.

469 Real-time qPCR performed on free-living mycelium, symbiotic tissues and fruiting bodies
470 showed a high level of *MiSSP8* expression both in mycorrhizal root tips and fruiting bodies
471 but not the free-living mycelium. This expression profile suggests an involvement of MiSSP8
472 in both symbiosis-related (i.e. formation of ectomycorrhiza) and non-symbiosis-related
473 processes (i.e. fruiting body formation). Both the ectomycorrhizal mantle sheath and the
474 fruiting body tissues are composed of pseudoparenchyma, a pseudo-tissue made of aggregated
475 hyphae that looks like the plant parenchyma (Brunner and Scheidegger, 1992 ; Peterson and
476 Farquhar, 1994). Ectomycorrhizae developed by *MiSSP8*-RNAi lines display a disorganized
477 fungal mantle and no Hartig net formation. We speculate that this phenotype results of the
478 lack of fungal aggregation. Hyphae from mantle are indeed glued together and embedded into
479 an extracellular material composed of glycoproteins and fungal polysaccharides (e.g. chitin, β
480 1-3 glucans) (Massicotte *et al.*, 1990; Dexheimer *et al.*, 1994). Previous studies propose a
481 sequential role of hydrophobins, repellent and polypeptides with a RGD motif (e.g. SRAP32),
482 in the aggregation of hyphae during mantle development in the ectomycorrhizal fungus
483 *Pisolithus tinctorius* (reviewed by Martin *et al.*, 1999).

484

485 **MiSSP8 is repetitive protein with a kexin cleavage site sharing similarities with other**
486 **repetitive proteins from saprotrophs**

487 Since *MiSSP8* displays high sequence similarity with only one *L. amethystina* gene, we
488 conclude that *MiSSP8* is a *Laccaria*-specific gene, upregulated both in symbiosis and in
489 fruiting bodies. These lineage-specific genes may have been formed *de novo* or may derived
490 from neofunctionalization of duplicated genes or from ancestral genes that have strongly
491 diverged due to selection pressure (Kohler *et al.*, 2015 ; Pellegrin *et al.*, 2015). However,
492 despite the absence of sequence similarities, a MCL (Markov Cluster Algorithm) analysis
493 performed on a set of 49 fungal genomes had previously retrieved 33 proteins containing a
494 similar motif as *MiSSP8* (Kohler *et al.*, 2015). With the current analysis, and using a different
495 search approach. we also identify additional fungal proteins harboring the same repetitive
496 motif than *MiSSP8* as well as a kexin endoprotease cleavage site (K/R)R (Mizuno *et al.*,
497 1988; Mizuno *et al.*, 1989). In addition, we showed this cleavage site is recognized *in vitro* by
498 yeast KEX2. Despite several trials, we were not able to detect the predicted released peptides
499 in ectomycorrhiza root tips or *L. bicolor* fruiting bodies (data not shown). This could be due
500 to post-translational modifications of the peptides or a fixation to extracellular components
501 such as fungal cell wall carbohydrates or glycoproteins. We can therefore only suggest that
502 the proteins containing the (DWRR)_n motif could be processed by kexin prior to their
503 secretion or go through post-translational modifications in order to become active and release
504 such peptides. Several fungal peptides are produced from KEX2-processed precursor proteins
505 (Le Marquer *et al.*, 2019) e.g., cyclic peptides with mycotoxic activity in Ascomycota such as
506 phomopsins (Ding *et al.*, 2016) or ustiloxins (Umemura *et al.*, 2014). On the other hand,
507 *Ustilago maydis* Rep1 protein is also cleaved by kexin-protease and has a structural role in the
508 fungal cell wall (Wösten *et al.*, 1996; Teertstra *et al.*, 2006). A 11 amino acid long peptide
509 processed by KEX2 in *Cryptococcus neoformans* is required for virulence and to activate the
510 sexual program (Homer *et al.*, 2016; Tian *et al.*, 2018). Since *MiSSP8*-RNAi lines are not
511 impaired in hyphal growth or fungal cell-wall sensitivity, it is unlikely that *MiSSP8* or its
512 derived peptides are involved in fungal cell wall structure. In addition, *MiSSP8* does not bind
513 to fungal cell wall sugars (data not shown). The precise role of *MiSSP8* and its derived
514 peptides in the development of the fungal mantle will require further research.

515 The fungal proteins identified in our study exhibit the (DW[K/R]R)_n motif at their C-termini
516 with a variable number of repetitions but they do not share sequence similarities at their N-
517 termini. Variations in number of tandem repeats is thought to provide functional diversity
518 (Verstrepen *et al*, 2005), suggesting that the identified DW[K/R]R-containing proteins might
519 be involved in various cellular processes and carry out different functions. If KEX2-
520 processed, the variable number of repeats would lead to different number of released peptides.
521 A comparative phylogenomics analysis of 49 fungal genomes revealed that ECM fungi have
522 evolved several times from saprotrophic ancestors, these being either white rot, brown rot or
523 soil decayers, by developing a set of symbiotic genes with rapid turnover, and in particular
524 gain of genes such as MiSSPs (Kohler *et al.*, 2015). Moreover, a recent comparative analysis
525 of five *Amanita* genomes, two ECM symbionts and three asymbiotic species, concluded that
526 several genetic components of the toolkit used by ECM symbionts is already encoded in the
527 genome of their saprotrophic relatives, explaining the recurrent emergence of the ECM
528 symbiosis over time (Hess *et al.*, 2018). Consistent with this finding, MiSSP8 shares
529 similarities with other saprotrophic proteins through its fungal-specific repetitive motif. Since
530 MiSSP8 is likely playing a role in the formation of the pseudoparenchyma of both non-
531 symbiotic (basidiocarp) and symbiotic (ECM) structures, we propose that MiSSP8 function,
532 initially required for *L. bicolor* fruiting body formation, has been recruited for the
533 establishment of the symbiosis. This highlights the dual use of the given secreted protein into
534 symbiotic and non-symbiotic processes. Our analysis also suggest that there are two
535 categories of MiSSPs: the orphan ones, such as MiSSP7 and the ones preexisting in
536 saprotrophic ancestors, such as MiSSP8.

537

538 In conclusion, we have characterized the Mycorrhiza induced Small Secreted Protein
539 of 8 kDa (MiSSP8) by combining functional and *in silico* approaches. We demonstrate that
540 MiSSP8 has a functional secretion signal peptide and it contains a repetitive motif containing
541 kexin cleavage sites recognized *in vitro* suggesting the protein might be cleaved in order to
542 become functional. Our data show that MiSSP8 or its derived peptides are decisive factors for
543 symbiosis establishment. The DWRR repetitive motif being also found in SSPs from

544 saprotrophic fungi, we propose that MiSSP8 or its derived peptides could have been initially
545 linked to fruiting body development by participating in pseudoparenchyma formation through
546 fungal hyphae aggregation before being recruited for symbiosis establishment.

547

548 **Acknowledgments**

549 This research was sponsored by the Genomic Science Program, US Department of Energy,
550 Office of Science, Biological and Environmental Research as part of the Plant-Microbe
551 Interfaces Scientific Focus Area (<http://pmi.ornl.gov>) and the Laboratory of Excellence
552 ARBRE (grant no. ANR-11-LABX-0002_ARBRE). The research was supported by the
553 Institut National de la Recherche Agronomique and the University of Lorraine (Ph.D.
554 scholarship to CP and YD). Both Région Lorraine Research council and the European Fund
555 for Regional Development give funding for the Functional Genomics Facilities at Institut
556 National de la Recherche Agronomique-GrandEst. Part of the work was supported by
557 Laboratoire Recherche Sciences Végétales - UPS CNRS, MetaToul (Metabolomics and
558 Fluxomics Facilities, Toulouse, France, www.metatoul.fr) and the French National
559 infrastructure for metabolomics and fluxomics, www.metabohub.fr, MetaboHUB-ANR-11-
560 INBS-0010. JR was an AgreenSkills Marie Skłodowska Curie postdoctoral fellow co-funded
561 by the European Commission (FP7-267196). We thank Barbara Montanini and Simone
562 Ottonello for sharing the pSUC-modified vectors. We thank Alexandre Kriznik from the
563 Platform of Biophysics and Structural Biology-UMS 2008 IBSLor (CNRS-INSERM-UL) for
564 his technical assistance in circular dichroism and isothermal calorimetry experiments.
565 Funding to A.P. and M.K. was provided by grants from Universidad Nacional de Quilmes,
566 Consejo Nacional de Investigaciones Científicas y Técnicas, and Agencia Nacional de
567 Promoción Científica y Tecnológica, Argentina.

568 **Authors contributions**

569 CVF and FM designed and managed the project; CP, YD, FG, MK, JR, VP, NFdF, AH, CVF
570 performed the experiments; CP, CVF, MK, AP, VP, NFdF analyzed the data; CP performed
571 the bioinformatic analysis; CP and CVF wrote the manuscript and all authors revised it.

572

573
574
575
576
577
578
579
580
581
582
583
584
585
586
587
588
589
590
591
592
593
594
595
596
597
598
599
600
601
602
603
604
605
606
607
608
609
610
611
612
613
614
615

References

1. **Akum, F. N., Steinbrenner, J., Biedenkopf, D., Imani, J., and Kogel, K.-H. 2015.** The *Piriformospora indica* effector PIIN_08944 promotes the mutualistic Sebacinalean symbiosis. *Front. Plant Sci.* 6:906
2. **Balestrini, R., and Kottke, I. 2016.** Structure and development of ectomycorrhizal roots. Pages 47–61 in: *Molecular Mycorrhizal Symbiosis*,
3. **Berg, G., Mahnert, A., and Moissl-Eichinger, C. 2014.** Beneficial effects of plant-associated microbes on indoor microbiomes and human health? *Front. Microbiol.* 5
4. **Berg, S., Pimenov, A., Palmer, C., Emmerson, M., and Jonsson, T. 2015.** Ecological communities are vulnerable to realistic extinction sequences. *Oikos.* 124:486–496
5. **Brundrett, M. C. 2009.** Mycorrhizal associations and other means of nutrition of vascular plants: Understanding the global diversity of host plants by resolving conflicting information and developing reliable means of diagnosis. *Plant Soil.* 320:37–77
6. **Brunner, I., and Scheidegger, C. 1992.** Ontogeny of synthesized *Picea abies* (L.) Karst.–*Hebeloma crustuliniforme* (Bull. ex St Amans) Qué. ectomycorrhizas. *New Phytol.* 120:359–369
7. **Buée, M., Reich, M., Murat, C., Morin, E., Nilsson, R. H., Uroz, S., and Martin, F. 2009.** 454 Pyrosequencing analyses of forest soils reveal an unexpectedly high fungal diversity. *New Phytol.* 184:449–456
8. **Daguerre, Y., Plett, J. M., and Veneault-Fourrey, C. 2017.** “Signaling pathways driving the development of ectomycorrhizal symbiosis,” in *Molecular Mycorrhizal Symbiosis*, ed. F. Martin (Hoboken, NJ: John Wiley & Sons, Inc), 141–157.
9. **de Castro, E., Sigrist, C. J. A., Gattiker, A., Bulliard, V., Langendijk-Genevaux, P. S., Gasteiger, E., Bairoch, A., and Hulo, N. 2006.** ScanProsite: Detection of PROSITE signature matches and ProRule-associated functional and structural residues in proteins. *Nucleic Acids Res.* 34
10. **Dexheimer, J., Gerard, J., and Genet, P. 1994.** Study of transformations of the root system of *Eucalyptus globulus* associated with *Pisolithus tinctorius*. I. Aptitude to mycorrhization of different kinds of roots. *Phytomorphology.* 44:235–245
11. **Ditengou, F. A., Müller, A., Rosenkranz, M., Felten, J., Lasok, H., van Doorn, M. M., Legué, V., Palme, K., Schnitzler, J.-P., and Polle, A. 2015.** Volatile signalling by sesquiterpenes from ectomycorrhizal fungi reprogrammes root architecture. *Nat. Commun.* 6:6279
12. **Doré, J., Perraud, M., Dieryckx, C., Kohler, A., Morin, E., Henrissat, B., Lindquist, E., Zimmermann, S. D., Girard, V., Kuo, A., et al. 2015.** Comparative genomics, proteomics and transcriptomics give new insight into the exoproteome of the basidiomycete *Hebeloma cylindrosporum* and its involvement in ectomycorrhizal symbiosis. *New Phytol.* 208:1169–1187

- 616 13. Drozdetskiy, A., Cole C, Procter J, Barton GJ. 2015. JPred4: a protein secondary
617 structure prediction server. *Nucleic Acids Res.* 43:389–394.
- 618 14. Felten, J., Kohler, A., Morin, E., Bhalerao, R. P., Palme, K., Martin, F., Ditengou,
619 F. A., and Legue, V. 2009. The Ectomycorrhizal Fungus *Laccaria bicolor* Stimulates
620 Lateral Root Formation in Poplar and Arabidopsis through Auxin Transport and
621 Signaling. *Plant Physiol.* 151:1991–2005
- 622 15. Fierer, N., Breitbart, M., Nulton, J., Salamon, P., Lozupone, C., Jones, R.,
623 Robeson, M., Edwards, R. A., Felts, B., Rayhawk *et al.* 2007. Metagenomic and
624 small-subunit rRNA analyses reveal the genetic diversity of bacteria, archaea, fungi,
625 and viruses in soil. *Appl. Environ. Microbiol.* 73:7059–7066
- 626 16. Frith, M. C., Saunders, N. F. W., Kobe, B., and Bailey, T. L. 2008. Discovering
627 sequence motifs with arbitrary insertions and deletions. *PLoS Comput. Biol.* 4
- 628 17. Genre, A., and Bonfante, P. 2012. The Interface Between Plants and Mycorrhizal
629 Fungi: Nutrient Exchange, Signaling and Cell Organization. Pages 39–49 in *The*
630 *Mycota, IX: Fungal Associations 2nd Ed*, B. Hock, Springer Berlin Heidelberg,
631 Berlin, Heidelberg.
- 632 18. Gietz, R. D., and Schiestl, R. H. 2008. High-efficiency yeast transformation using the
633 LiAc / SS carrier DNA / PEG method. *Nat. Protoc.* 2:31–35
- 634 19. Hess, J., Skrede, I., Chaib De Mares, M., Hainaut, M., Henrissat, B. and Pringle,
635 A. 2018. Rapid Divergence of Genome Architectures Following the Origin of an
636 Ectomycorrhizal Symbiosis in the Genus *Amanita*. *Mol. Biol. Evol.*
637 doi:10.1093/molbev/msy179
- 638 20. Homer CM, Summers DK, Goranov AI, Clarke SC, Wiesner DL, Diedrich JK, *et*
639 *al.* 2016. Intracellular Action of a Secreted Peptide Required for Fungal Virulence.
640 Cell host and microbe. 19(6):849–64.
- 641 21. Jacobs, K. A., Collins-Racie, L. A., Colbert, M., Duckett, M., Golden-Fleet, M.,
642 Kelleher, K., Kriz, R., La Vallie, E. R., Merberg, D., Spaulding, V. *et al.* 1997. A
643 genetic selection for isolating cDNAs encoding secreted proteins. *Gene.* 198:289–296
- 644 22. Jacobs, K. A., Collins-Racie, L. A., Colbert, M., Duckett, M., Golden-Fleet, M.,
645 Kelleher, K., Kriz, R., La Vallie, E. R., Merberg, D., Spaulding, V. *et al.* 1997. A
646 genetic selection for isolating cDNAs encoding secreted proteins. *Gene.* 198:289–296
- 647 23. Kemppainen, M. J., and Pardo, A. G. 2010. pHg/pSILBA γ vector system for
648 efficient gene silencing in homobasidiomycetes: Optimization of ihpRNA - Triggering
649 in the mycorrhizal fungus *Laccaria bicolor*. *Microb. Biotechnol.* 3:178–200
- 650 24. Kemppainen, M., Circosta, A., Tagu, D., Martin, F., and Pardo, A. G. 2005.
651 Agrobacterium-mediated transformation of the ectomycorrhizal symbiont *Laccaria*
652 *bicolor* S238N. *Mycorrhiza.* 16:19–22
- 653 25. Kemppainen, M., Duplessis, S., Martin, F., and Pardo, A. G. 2008. T-DNA
654 insertion, plasmid rescue and integration analysis in the model mycorrhizal fungus
655 *Laccaria bicolor*. *Microb. Biotechnol.* 1:258–269
- 656 26. Kemppainen, M., Duplessis, S., Martin, F., and Pardo, A. G. 2009. RNA silencing
657 in the model mycorrhizal fungus *Laccaria bicolor*: Gene knock-down of nitrate

- 658 reductase results in inhibition of symbiosis with *Populus*. *Environ. Microbiol.*
659 11:1878–1896
- 660 27. **Kloppholz, S., Kuhn, H., and Requena, N. 2011.** A secreted fungal effector of
661 *Glomus intraradices* promotes symbiotic biotrophy. *Curr. Biol.* 21:1204–1209
- 662 28. **Kohler, A., Kuo, A., Nagy, L. G., Morin, E., Barry, K. W., Buscot, F., Canbäck,**
663 **B., Choi, C., Cichocki, N., Clum, A., et al. 2015.** Convergent losses of decay
664 mechanisms and rapid turnover of symbiosis genes in mycorrhizal mutualists. *Nat.*
665 *Genet.* 47:410–415
- 666 29. **Krause, K., Henke, C., Asimwe, T., Ulbricht, A., Klemmer, S., Schachtschabel,**
667 **D., Boland, W., and Kothe, E. 2015.** Biosynthesis and secretion of indole-3-acetic
668 acid and its morphological effects on *Tricholoma vaccinum*-spruce ectomycorrhiza.
669 *Appl. Environ. Microbiol.* 81:7003–7011
- 670 30. **Kües, U., Navarro-González, M. 2015.** How do Agaricomycetes shape their fruiting
671 bodies? 1. Morphological aspects of development. *Fungal Biology Reviews.* 29: 63-97
- 672 31. **Lakkireddy, K., Navarro-González, M., Velagapudi, R., and Kües, U. 2011.**
673 Proteins expressed during hyphal aggregation for fruiting body formation in
674 basidiomycetes. in: Proceedings of the 7th International Conference on Mushroom
675 Biology and Mushroom Products (ICMBMP7).
- 676 32. **Le Marquer, M., San Clemente, H., Roux, C., Savelli, B., and Frei dit Frey N.**
677 **2019.** Identification of new signalling peptides through a genome-wide survey of 250
678 fungal secretomes. *BMC Genomics.* 20:64. <https://doi.org/10.1186/s12864-018-5414-2>
- 679 33. **Lindahl, B. D., and Tunlid, A. 2015.** Ectomycorrhizal fungi - potential organic
680 matter decomposers, yet not saprotrophs. *New Phytol.* 205:1443–1447
- 681 34. **Liu, Y., Guang, G., Mitsukawa, N., Oosumi, T., and Whittier, R. F. 1995.** Efficient
682 isolation and mapping of *Arabidopsis thaliana* T-DNA insert junctions by thermal
683 asymmetric interlaced PCR. *Plant J.* 8:457–463
- 684 35. **Lo Presti, L., Lanver, D., Schweizer, G., Tanaka, S., Liang, L., Tollot, M.,**
685 **Zuccaro, A., Reissmann, S., and Kahmann, R. 2015.** Fungal Effectors and Plant
686 Susceptibility. *Annu. Rev. Plant Biol.* 66:513–545
- 687 36. **Martin, F., Aerts, A., Ahrén, D., Brun, A., Danchin, E. G. J., Duchaussoy, F.,**
688 **Gibon, J., Kohler, A., Lindquist, E., Pereda et al. 2008.** The genome of *Laccaria*
689 *bicolor* provides insights into mycorrhizal symbiosis. *Nature.* 452:88–92
- 690 37. **Martin, F., Kohler, A., Murat, C., Veneault-Fourrey, C., and Hibbett, D. S. 2016.**
691 Unearthing the roots of ectomycorrhizal symbioses. *Nat. Rev. Microbiol.* 14:760–773
- 692 38. **Martin, F., Laurent, P., de Carvalho, D., Voiblet, C., Balestrini, R., Bonfante, P.,**
693 **and Tagu, D. 1999.** Cell wall proteins of the ectomycorrhizal basidiomycete
694 *Pisolithus tinctorius*: identification, function, and expression in symbiosis. *Fungal*
695 *Genet. Biol.* 27:161–174
- 696 39. **Massicotte, H. B., Peterson, R. L., Ackerley, C. A., and Melville, L. H. 1990.**
697 Structure and ontogeny of *Betula alleghaniensis* – *Pisolithus tinctorius*
698 ectomycorrhizae. *Can. J. Bot.* 68:579–593

- 699 40. Mizuno, K., Nakamura, T., Ohshima, T., Tanaka, S., and Matsuo, H. 1988. Yeast
700 KEX2 gene encodes an endopeptidase homologous to subtilisin-like serine proteases.
701 *Biochem. Biophys. Res. Commun.* 156:246–254
- 702 41. Mizuno, K., Nakamura, T., Ohshima, T., Tanaka, S., and Matsuo, H. 1989.
703 Characterization of KEX2-encoded endopeptidase from yeast *Saccharomyces*,
704 *cerevisiae*. *Biochem. Biophys. Res. Commun.* 159:305–311
- 705 42. Mullins, E. D., Chen, X., Romaine, P., Raina, R., Geiser, D. M., and Kang, S.
706 2001. *Agrobacterium*-Mediated Transformation of *Fusarium oxysporum*: An Efficient
707 Tool for Insertional Mutagenesis and Gene Transfer. *Phytopathology.* 91:173–180
- 708 43. Murashige, T., and Skoog, F. 1962. A Revised Medium for Rapid Growth and Bio
709 Assays with Tobacco Tissue Cultures. *Physiol. Plant.* 15:473–497
- 710 44. Paschlewski and Paschlewskia. 1974. Studies on symbiotic properties of mycorrhizal
711 fungi of pine (*Pinus sylvestris* L.) with the aid of the method of mycorrhizal synthesis
712 in pure culture on agar. (Translated into English by Royal Dzieciolowski). Warsaw,
713 Pol. For. Res. Inst.
- 714 45. Pellegrin, C., Morin, E., Martin, F. M., and Veneault-Fourrey, C. 2015.
715 Comparative analysis of secretomes from ectomycorrhizal fungi with an emphasis on
716 small-secreted proteins. *Front. Microbiol.* 6
- 717 46. Peterson, A. R. L., and Farquhar, M. L. 1994. Mycorrhizas : Integrated
718 Development between Roots and Fungi. *Mycologia.* 86:311–326
- 719 47. Pfaffl, M. W. 2001. A new mathematical model for relative quantification in real-time
720 RT-PCR. *Nucleic Acids Res.* 29:45e–45
- 721 48. Plett, J. M., and Martin, F. 2015. Reconsidering mutualistic plant-fungal interactions
722 through the lens of effector biology. *Curr. Opin. Plant Biol.* 26:45–50
- 723 49. Plett, J. M., Daguerre, Y., Wittulsky, S., Vayssieres, A., Deveau, A., Melton, S. J.,
724 Kohler, A., Morrell-Falvey, J. L., Brun, A., Veneault-Fourrey, C. *et al.* 2014.
725 Effector MiSSP7 of the mutualistic fungus *Laccaria bicolor* stabilizes the *Populus*
726 JAZ6 protein and represses jasmonic acid (JA) responsive genes. *Proc. Natl. Acad.*
727 *Sci.* 111:8299–8304
- 728 50. Plett, J. M., Kemppainen, M., Kale, S. D., Kohler, A., Legué, V., Brun, A., Tyler,
729 B. M., Pardo, A. G., and Martin, F. 2011. A secreted effector protein of *Laccaria*
730 *bicolor* is required for symbiosis development. *Curr. Biol.* 21:1197–1203
- 731 51. Plett, J. M., Tisserant, E., Brun, A., Morin, E., Grigoriev, I. V., Kuo, A., Martin,
732 F., and Kohler, A. 2015. The Mutualist *Laccaria bicolor* Expresses a Core Gene
733 Regulon During the Colonization of Diverse Host Plants and a Variable Regulon to
734 Counteract Host-Specific Defenses. *Mol. Plant-Microbe Interact.* 28:261–273
- 735 52. Ruxton, G.D., and Beauchamp, G. (2008) ‘Time for some a priori thinking about
736 post hoc testing’, *Behavioral Ecology*, 19(3), pp. 690-693. doi:
737 10.1093/beheco/arn020.
- 738 53. Shen, A., Lupardus, P. J., Morell, M., Ponder, E. L., Sadaghiani, A. M., Garcia,
739 K. C., and Bogyo, M. 2009. Simplified, enhanced protein purification using an
740 inducible, autoprocessing enzyme tag. *PLoS One.*
741 4:doi.org/10.1371/journal.pone.0008119

- 742 54. **Teertstra WR, Deelstra HJ, Vranes M, Bohlmann R, Kahmann R, et al. (2006).**
743 Repellents have functionally replaced hydrophobins in mediating attachment to a
744 hydrophobic surface and in formation of hydrophobic aerial hyphae in *Ustilago*
745 *maydis*. *Microbiology* 152: 3607–3612.
- 746 55. **Tian X., He G. J., Hu P., Chen L., Tao C., Cui Y. L., et al. (2018).** Cryptococcus
747 neoformans sexual reproduction is controlled by a quorum sensing peptide. *Nat.*
748 *Microbiol.* 3 698–707. 10.1038/s41564-018-0160-4
- 749 56. **Umemura M. et al. (2014).** Characterization of the biosynthetic gene cluster for the
750 ribosomally synthesized cyclic peptide ustiloxin B in *Aspergillus flavus*. *Fungal*
751 *Genet. Biol.*, 68, 23–30.
- 752 57. **Uroz, S., Buée, M., Murat, C., Frey-Klett, P., and Martin, F. 2010.** Pyrosequencing
753 reveals a contrasted bacterial diversity between oak rhizosphere and surrounding soil.
754 *Environ. Microbiol. Rep.* 2:281–288
- 755 58. **van Der Heijden, M. G. A., Klironomos, J. N., and Ursic, M. 1998.** Mycorrhizal
756 fungal diversity determines plant biodiversity, ecosystem variability and productivity.
757 *Nature.* 396:69–72
- 758 59. **Vandesompele, J., De Preter, K., Pattyn, F., Poppe, B., Van Roy, N., De Paepe,**
759 **A., and Speleman, rank. 2002.** Accurate normalization of real-time quantitative RT-
760 PCR data by geometric averaging of multiple internal control genes. *Genome Biol.*
761 3:34–1
- 762 60. **Vayssières, A., Pěňčík, A., Felten, J., Kohler, A., Ljung, K., Martin, F., and**
763 **Legué, V. 2015.** Development of the Poplar-*Laccaria bicolor* Ectomycorrhiza
764 Modifies Root Auxin Metabolism, Signaling, and Response. *Plant Physiol.* 169:890–
765 902
- 766 61. **Verstrepen, K., Jansen, A., Lewitter, F. and Fink, G. 2005.** Intragenic tandem
767 repeats generate functional variability. *Nature Genet.* 37:986–990.
- 768 62. **Wawra, S., Fesel, P., Widmer, H., Timm, M., Seibel, J., Leson, L., Kessler, L.,**
769 **Nostadt, R., Hilbert, M., Langen, G. et al. 2016.** The fungal-specific β -glucan-
770 binding lectin FGB1 alters cell-wall composition and suppresses glucan-triggered
771 immunity in plants. *Nat. Commun.* 7:13188
- 772 63. **Welch, B. L. (1947).** "The generalization of "Student's" problem when several
773 different population variances are involved". *Biometrika.* 34 (1–2): 28–35.
774 doi:10.1093/biomet/34.1-2.28. MR 0019277.
- 775 64. **Wödsten, H. A. B., Bohlmann, R., Eckerskorn, C., Lottspeich, F., Bolker, M. and**
776 **Kahmann, R. (1996).** A novel class of small amphipathic peptides affect aerial
777 hyphal growth and surface hydrophobicity in *Ustilago maydis*. *EMBO J* 15, 4274–4281
778

779 **Legends of Figures**

780 **Figure 1: MiSSP8 is a secreted repeat-containing protein highly expressed in**
781 **ectomycorrhizal root tips and fruiting body tissues.**

782 (A) Real-time qPCR time course performed on *Laccaria bicolor* extraradical mycelium
783 (ExM), free-living mycelium (FLM) and during development of *Populus tremula* x *alba* ECM
784 root tips. Expression of *MiSSP8* in FLM was set as a reference. Error bars represent standard
785 deviation from three biological replicates.

786 (B) Real-time qPCR analysis on the expression of *MiSSP8* versus two reference genes in the
787 fruiting body of *L. bicolor*, the cap and stipe, at both early and late stages of development.
788 Stars indicate significant differences (p-value cut-off < 0.05) using Welch t-test (Welch,
789 1947). Error bars represent standard deviation from three biological replicates.

790 (C) *MiSSP8* sequence, domain organization and hydrophobicity score as obtained by
791 ProtScale using the amino-acid scale from Kyle and Doolittle (1982) with a window size of 5.

792 (D) Yeast signal trap assay shows that the signal peptide predicted in *MiSSP8* sequence is
793 functional in yeast. *Saccharomyces cerevisiae* was transformed either with empty vector
794 control (top left), mature *MiSSP8* (lacking its signal peptide) fused to mature invertase
795 (*MiSSP8* Δ 1-20::Invertase, top right), full-length invertase (with its signal peptide, bottom
796 left) or full length *MiSSP8* fused to mature invertase (*MiSSP8*::Invertase, bottom right).
797 Transformed yeasts were plated on growth medium containing sucrose as the sole source of
798 carbon.

799

800 **Figure 2: The DW[K/R]R proteins possess a repetitive structure and are likely secreted.**

801 The modular structure of the proteins is shown. Protein domains have been identified by
802 PROSITE and signal peptides are predicted by SignalP v4.1.

803

804 **Figure 3: MiSSP8-repetitive motif is found in proteins from saprotrophic and**
805 **ectomycorrhizal fungi.**

806 (A) Size distribution (in amino acids) of the DW[K/R]R-containing proteins within the
807 different fungal lifestyles identified.

808 **(B)** Number of repetitions identified in the DW[K/R]R-containing proteins.

809 **(C)** Identification of the DWRR motif by GLAM2 software. The set of 38 sequences retrieved
810 with PS-Scan has been submitted to GLAM2 run with default parameters.

811

812

813 **Figure 4. Recombinant MiSSP8 is cleaved by KEX2 protease *in vitro*.**

814 **(A)** Visualization of proteolytic digests of recombinant MiSSP8 and MiSSP7 proteins by
815 recombinant KEX2 protease, separated on Coomassie-stained-polyacrylamide gels. A time
816 course over 1, 2, 4 and 6h of incubation was performed. Sizes are indicated in kDa. MiSSP7
817 is used as negative control since it is not a putative substrate for KEX2 protease.+ and -
818 indicate the presence or absence of KEX2, respectively.

819 **(B)** Detected peptides by LC-MS/MS after 4h of digestion by the recombinant KEX2 protease
820 of the MiSSP8 protein. Theoretical formed peptides are DSDWRR and DSDVD but
821 additional combinations of cleavages were hypothesized. The transitions selected for each
822 peptide were: m/z 522.5>185 (DSDW, RT: 5.0 min), 550.5>175 (DSDVD, RT: 4.5 min),
823 678.5>254 (RDSDW, RT: 5.0 min), 678.5>361 (DSDWR, RT: 4.4 min), 834.5>517
824 (DSDWRR, RT: 4.0 min), 834.5>361 (RDSDWR, RT: 4.0 min), 834.5>313 (RRDSDW, RT:
825 4.0 min). Peak height intensity is measured in counts per second (cps). Mean of 3 independent
826 replicates, standard error of the mean is reported.

827

828 **Figure 5: Knockdown of *MiSSP8* impairs the establishment of ectomycorrhizal**
829 **symbiosis.**

830 **(A)** Expression was measured by qRT-PCR. All values are shown as mean \pm standard
831 deviation; n = 3. Stars indicate that expression is statistically different than control line based
832 on a non-parametric Kruskal-Wallis test followed by a Games-Howell post-hoc test (Ruxton
833 and Beauchamp, 2008). Adjusted p-value (FDR) cut-off = 0.05. ev indicates fungal lines
834 transformed with an empty vector (i.e. negative control).

835 **(B)** Knockdown of *MiSSP8* strongly decreases the number of ectomycorrhizal root tips
836 compared to the wild-type strain or the empty vector controls. Percentage of poplar (*Populus*

837 *tremula x alba*) mycorrhizal root tips formed by wild-type *L. bicolor* S238N and two empty
838 vector transformation controls (ev7 and 9) versus four independent *L. bicolor* *MiSSP8*-RNAi
839 lines. All values are shown as mean \pm standard deviation; n=25; Stars indicate significant
840 difference from wild-type, ev7 and ev9 using t-test and a p-value cut-off < 0.05 .

841 (C) Transversal section of ectomycorrhizal root tips formed by ev7 control transformant line
842 and *MiSSP8*-RNAi line 3. The *MiSSP8*-RNAi line 3 displays a loose mantle and no Hartig net
843 compared to the empty vector control strain (ev7). Scale bars: 10 μ m. Propidium iodide stains
844 plant cell walls and nuclei (red) and WGA-Alexa 488 stains fungal cell walls (green). Green
845 signal in root cortical cells correspond to aspecific WGA-Alexa 488 fixation to plant cell
846 walls and not to fungal cells.

847

848 **Figure S1: Fruiting body of *L. bicolor* at two different developmental stages.** The cap and
849 stipe of fruiting bodies from *L. bicolor* were harvested at early and late developmental stages
850 in order to study the expression of *MiSSP8* during the development of the fruiting body.

851

852 **Figure S2: *In silico* prediction and experimental validation of *MiSSP8* secondary**
853 **structure.** (a) Secondary structure of *MiSSP8* as predicted by the JPred 4 server (Drozdetskiy
854 *et al*, 2015). (b) Analysis of recombinant *MiSSP8* secondary structure by circular dichroism.

855

856 **Figure S3: Correlation between protein size sequences and occurrence of the**
857 **DWRR/DWRR-like motif.** No correlation found between the size of the DW[K/R]R protein
858 sequences identified and the number of motifs they contain (A), even after removing the
859 outliers (B).

860

861 **Figure S4: Spectrum obtained for the peptide DSDWR in LC-MS/MS.** The selected
862 precursor ion (m/z 678.6) is corresponding to the peptide DSDWR (M+H)⁺; after
863 fragmentation (CE 40V), y ions are observed as predicted in Protein Prospector (m/z 175.1;
864 361.1; 476.2; 563.2; 678.2).

865

866 **Figure S5. *L. bicolor missp8* RNAi mutants are not impaired in their saprotrophic**
867 **growth in both control medium (P5) or under cell-wall stress conditions.**

868 Viability of *MiSSP8* RNAi lines was assessed by growing the different strains used (Wild-
869 type (WT), empty vector control (ev7) and the four RNAi lines generated on either control
870 medium (P5) or under cell-wall stress condition (Congo Red).

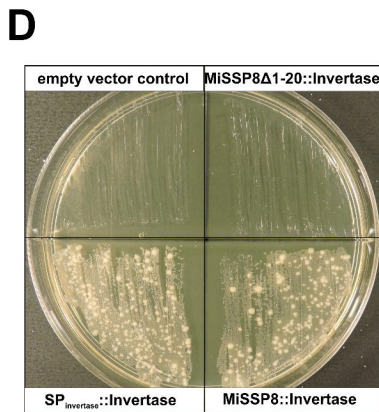
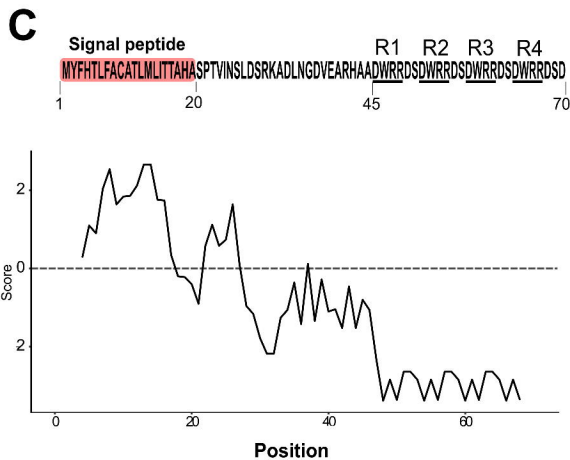
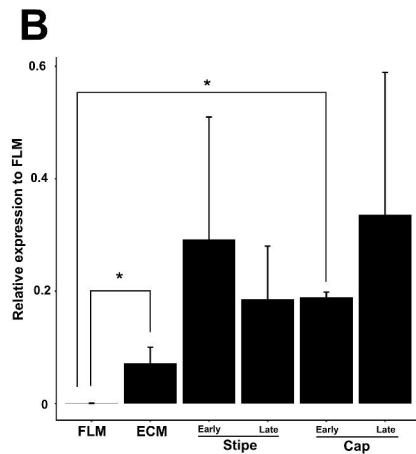
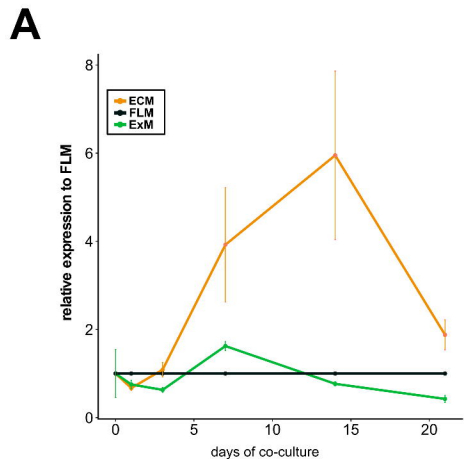
871

872 **Supplementary Table S1:** List of genomes scanned and proteins sequences containing from
873 two to twenty repetitions of the DW[K/R]R motif.

874

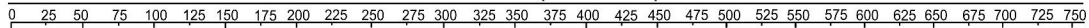
875 **Supplementary Table S2:** Molecular analysis of *Laccaria bicolor* *MiSSP8*-RNAi lines.
876 Molecular analysis of the four RNAi lines generated expressing RNAi hairpin targeting the
877 *MiSSP8* encoding transcript.

878



Species / Protein ID
 ■ Signal Peptide ■ DWRR/DWRR-like motif

Size (amino acids)



Ectomycorrhizal
Arbuscular mycorrhiza

Brown rot

White rot

Litter decayers

Other wood decayers

Laccaria bicolor / 388224 / MISSP8

Hebeloma cylindrosporum / 440029

Laccaria amethystina / 676588

Laccaria amethystina / 1718616

Laccaria bicolor / 334723

Rhizophagus irregularis / 46777

Gloeophyllum trabeum / 109288

Neolentinus lepideus / 1095641

Gloeophyllum trabeum / 141070

Galerina marginata / 204523

Punctularia strigosozonata / 115989

Schizophyllum commune H4-8 / 2611276

Schizophyllum commune H4-8 / 2745165

Schizophyllum commune / 2613917

Schizophyllum commune H4-8 / 2705922

Stereum hirsutum / 107311

Auriculariopsis delicata / 1302180

Pleurotus ostreatus / 114050

Pleurotus ostreatus / 171464

Amanita thiersii / 5213

Pleurotus ostreatus / 1091723

Agaricus bisporus / 88475

Exidia glandulosa / 774536

Exidia glandulosa / 642657

Exidia glandulosa / 759788

Auriculariopsis ampla / 5658320

Auriculariopsis ampla / 573463

Auriculariopsis ampla / 57527

Botryobasidium botryosum / 25997

Schizopora paradoxa / 936556

Plicaturopsis crispa / 180022

Hypholoma sublateralitium / 36958

Hypholoma sublateralitium / 202128

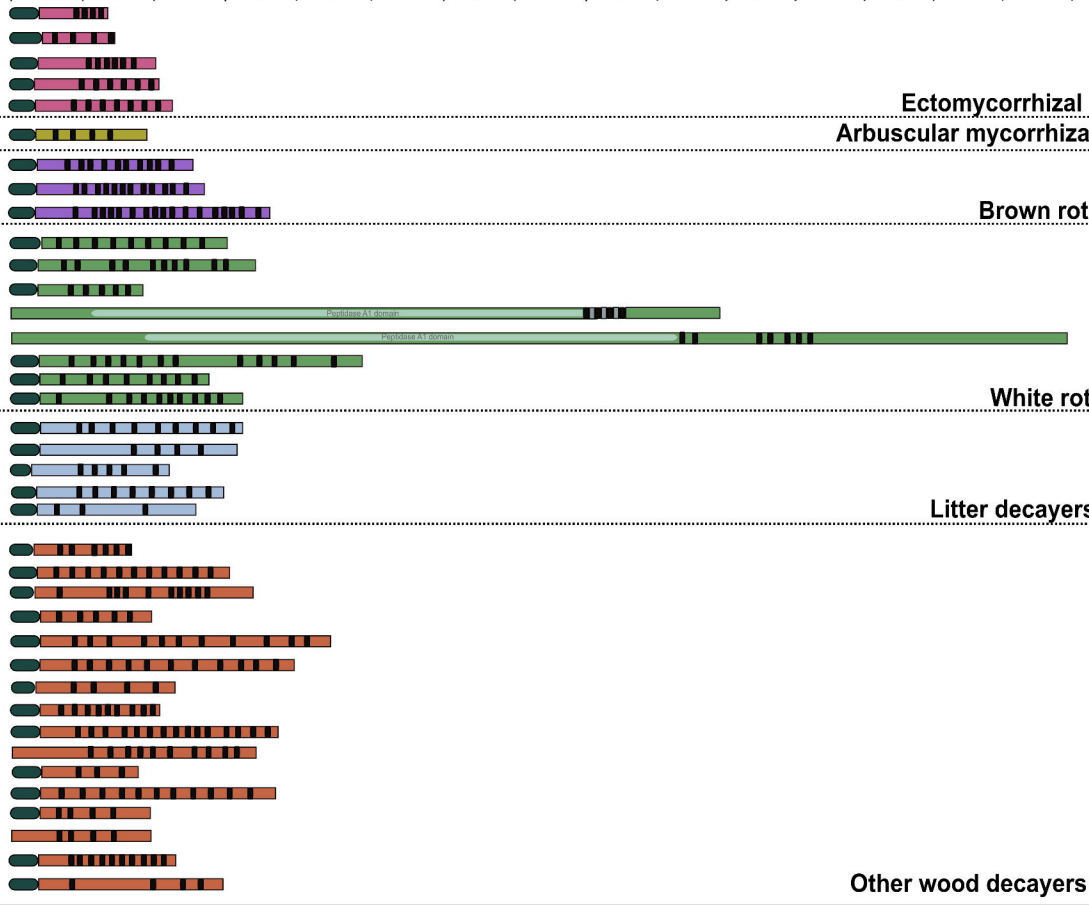
Gymnopus luxurians / 242026

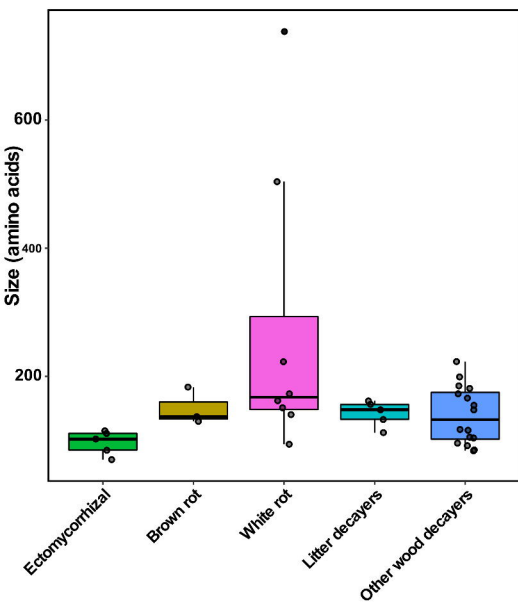
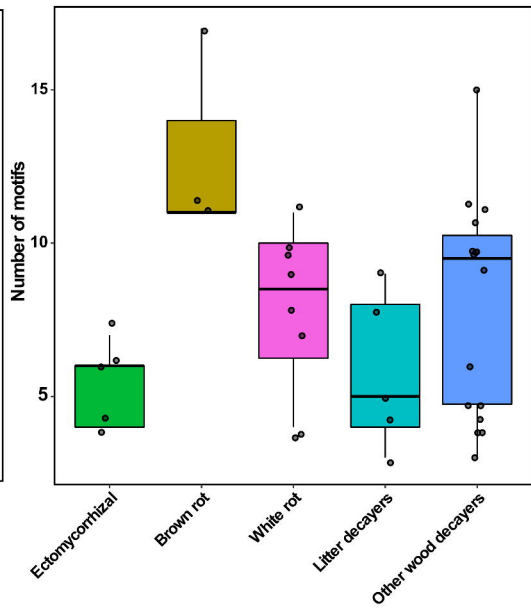
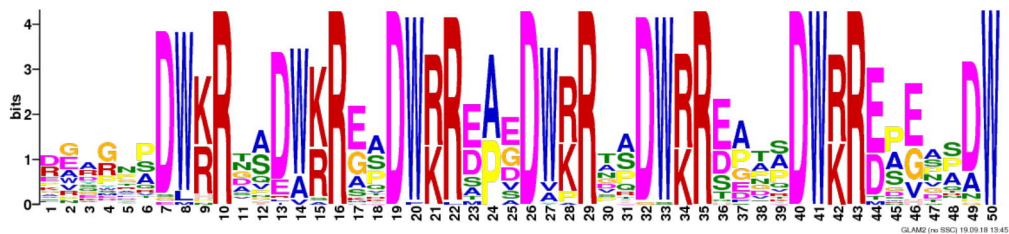
Gymnopus luxurians / 239794

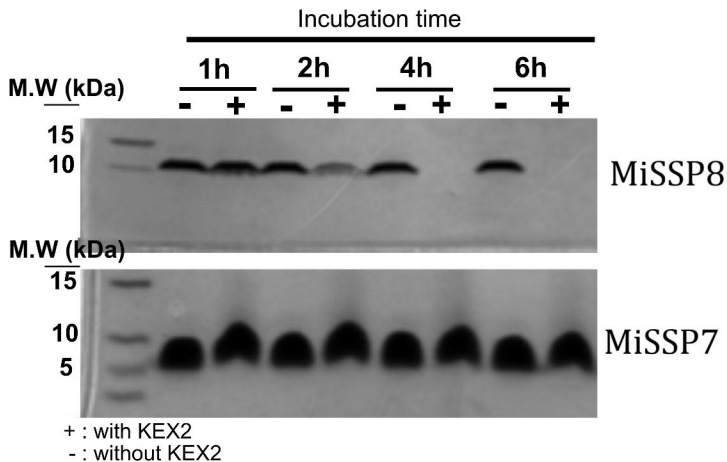
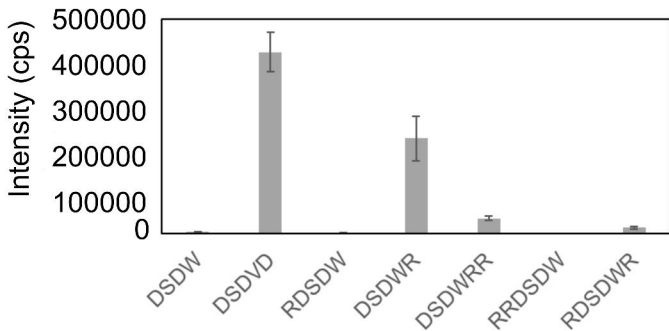
Gymnopus luxurians / 98464

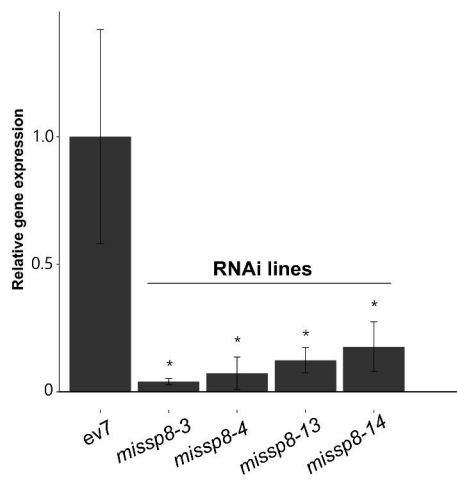
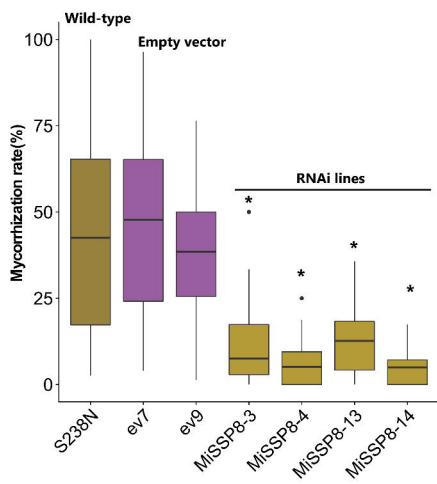
Fistulina hepatica / 75093

Bjerkandera adusta / 30962



A**B****C**

A**B**

A**B****C**